Analyst

Accepted Manuscript

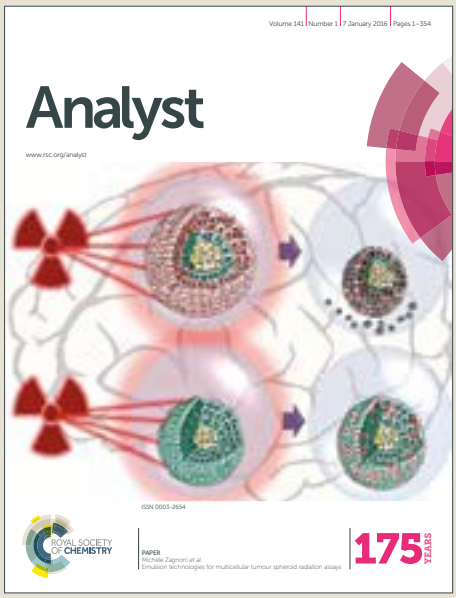

ROYAL SOCIETY OF CHEMISTRY

rsc.li/analyst

View Article Online
DOI: 10.1039/C7AN01438D

Terahertz spectroscopy for the isothermal detection of bacterial DNA by magnetic bead-based rolling circle amplification

Xiang Yang, Ke Yang, Xiang Zhao, Zhongquan Lin, Zhiyong Liu, Sha Luo, Yang Zhang, Yunxia Wang, Weiling Fu*

Department of Laboratory Medicine, Southwest Hospital, Third Military Medical University, Chongqing 400038, China

Corresponding Author

*(W.-L.F) E-mail: weiling_fu@126.com

View Article Online
DOI: 10.1039/C7AN01438D

ABSTRACT:

The demand for rapid and sensitive bacterial detection is continuously increasing due to the significant requirements of various applications. In this study, a terahertz (THz) biosensor based on rolling circle amplification (RCA) was developed for the isothermal detection of bacterial DNA. The synthetic bacterium-specific sequence of 16S rDNA hybridized with a padlock probe (PLP) that contains a sequence fully complementary to the target sequence at the 5' and 3' ends. The linear PLP was circularized by ligation to form a circular PLP upon recognition of the target sequence; then, the capture probe (CP) immobilized on magnetic beads (MBs) acted as a primer to initialize RCA. As DNA molecules are much less absorptive than water molecules in the THz range, the RCA products on the surface of the MBs cause a significant decrease in THz absorption, which can be sensitively probed by THz spectroscopy. Our results showed that 0.12 fmol of synthetic bacterial DNA and 0.05 ng/μL of genomic DNA could be effectively detected using this assay. In addition, the specificity of this strategy was demonstrated by its low signal response to interfering bacteria. The proposed strategy not only represents a new method for the isothermal detection of the target bacterial DNA but also provides a general methodology for sensitive and specific DNA biosensing using THz spectroscopy.

Key words: Terahertz spectroscopy; bacterial analysis; biosensor; rolling circle amplification

View Article Online
DOI: 10.1039/C7AN01438D

Introduction

The terahertz (THz) region refers to the 0.1 to 10 THz frequency range of the electromagnetic spectrum. This range remained relatively unexplored in the biological sciences until the advent of powerful sources and detectors in the 1980s.[1] The photon energy level of THz radiation largely coincides with that of low-frequency biomolecular motions, including vibration, rotation and translation of the molecular skeleton.[2] Due to its unique frequency range, THz radiation possesses excellent sensitivity to the water content and tiny structural changes of biomaterials.[3] As a result, THz spectroscopy has proven to be an effective tool in various biomedical applications, such as solvation dynamics investigations,[4] tablet coating characterization,[5] and intermolecular interaction monitoring.[6] Notably, a pioneer study has demonstrated the feasibility of quantitative DNA analysis in aqueous solution using THz spectroscopy with a minimum sample volume of 10 μL.[7] The THz absorption coefficients of DNA solutions decreased linearly with increasing DNA concentration due to the replacement of highly absorbing water molecules by much less absorbing DNA molecules. This phenomenon can be exacerbated by the retardation of water dynamics in the dynamical hydration shell around DNA molecules.[8] Consequently, the effects of water replacement and the change of water THz modes lead to a decreased THz signal with increasing DNA concentration, which implies another exciting possibility of developing THz biosensors for the label-free quantitative analysis of DNA solutions.

Rolling circle amplification (RCA) is an isothermal and efficient nucleic acid amplification method with high specificity and simplicity. Before amplification, the target DNA can serve as a ligation template to circularize a linear padlock probe (PLP) by joining their fully complementary ends.[9] The circularized PLP can then be used as an amplification template in combination with a primer to initialize RCA. Unlike the polymerase chain reaction (PCR), which requires a thermal cycler and thermostable DNA polymerases,[9] RCA can be easily conducted under isothermal conditions (from room temperature to 37°C). In addition, this user-friendly method is more resistant to

carry-over contamination and non-specific amplification than PCR and can be performed on a solid support.[10] Thus, solid-phase RCA can be realized by the surface-tethered primer or target on multiple surfaces, such as glass, microbeads or microfluidic chips.[11] Therefore, solid-phase-RCA strategies have been coupled to various optical biosensors and immunoassays to be utilized as a signal amplification element.[9] Our previous studies combined RCA with surface plasmon resonance (SPR) biosensors to detect bacterial DNA with surface-immobilized capture probes (CPs; primers) on gold nanoparticles and on gold film.[12, 13]

However, when coupling RCA with THz spectroscopy, an obvious issue lies in the absorption interference of complex components in sample matrices. THz absorption spectra of DNA solutions are generally monotonically increasing curves that exhibit no specific features (absorption signatures) at room temperature and should be compared based on the contributions of all components.[7] Meanwhile, biomolecules are less absorptive than water molecules in the THz range, and their aqueous solutions generally have lower THz absorption than water.[14] In contrast, ions such as Mg, K, and H tend to increase the THz absorption of aqueous solutions,[15-17] possibly obscuring the spectral changes. Therefore, the RCA product needs to be separated from complex sample matrix components (deoxyribonucleosides (dNTPs), ions, enzyme and buffer) to reduce the background signal prior to THz measurements. Due to their physical and chemical stability, magnetic beads (MBs) have been extensively incorporated into various bioassays for the isolation and purification of cells and molecules.[18, 19] For instance, MBs have been utilized to separate RCA products from complex sample matrix components via conjugated complementary DNA probes that bind to the periodic patterns of RCA products.[20] In addition, the excellent biocompatibility of MBs, such as their lack of inhibition of enzyme activity, makes them ideal biosensing assay platforms for solid-phase reactions. Therefore, RCA primers could also be immobilized onto MBs for the subsequent hybridization with circularized templates to initialize surface DNA amplification on MBs.[21] Taking advantage of this strategy, RCA products could be

directly enriched and magnetically separated from sample matrix components, eliminating the extra hybridization procedure.

In this study, a THz biosensing strategy based on RCA that combines the aforementioned techniques is proposed for the isothermal detection of bacterial DNA. In this protocol, the target sequence is captured by linear PLPs to form circular PLPs; then, the biotinylated CPs immobilized on streptavidin-coated MBs act as primers to initialize an *in situ* solid-phase RCA reaction on the MBs upon recognition of the circularized PLPs. This strategy enables a simple separation of DNA products by magnetic purification after RCA, thus eliminating the interferences from sample matrix components for subsequent THz measurements. *Escherichia coli* was selected as the target organism, and 0.12 fmol of synthetic bacterial DNA and 0.05 ng/μl of genomic DNA were effectively detected by this method within 40 min of amplification. The specificity of the proposed strategy was also evaluated by testing the THz response to interfering bacteria. Our results clearly illustrated the potential of THz spectroscopy for sensitive and specific DNA detection by MB-based RCA.

Experimental

Chemicals, reagents and materials

All oligonucleotides used in this study (Table 1) were synthesized and purified via high-performance liquid chromatography (HPLC) by Sangon Biotech (Shanghai, China). *E. coli* DNA ligase, exonuclease I, exonuclease III, QuickCut™ *Bam*HI, QuickCut™ *Eco*RI, QuickCut™ *Hind*III, DL2000 Maker and a TaKaRa MiniBEST Bacteria Genomic DNA Extraction Kit Ver.3.0 were purchased from Takara (Dalian, China). Phi 29 DNA polymerase, dNTPs and SYBR Green II dye were from Thermo Scientific (USA). Streptavidin-coated MBs with a diameter of 1 μm (Dynabeads MyOne Streptavidin C1) were from Dynal Biotech, Invitrogen (MA, USA). *E. coli* ATCC 25922, *Acinetobacter baumannii* ATCC 19606 and *Pseudomonas aeruginosa* ATCC 27853 were obtained from Southwest Hospital (Chongqing, China). All chemicals

employed were of analytical reagent grade. High-purity deionized water prepared by a Milli-Q water purification system (Millipore Corp., Bedford, USA) was used throughout the experiments.

Ligation and exonuclease treatment in solution

First, the PLP (100 nM) was hybridized with the target sequence (10 nM) in a 20 μL reaction mixture (30 mM Tris-HCl (pH 8.0), 4 mM $MgCl_2$, 10 mM $(NH_4)_2SO_4$, 1.2 mM EDTA, and 100 μM NAD). The mixture was denatured at 95 °C for 5 min and then cooled to 4 °C. Subsequently, the mixture was incubated at 60 °C for 30 min before 5 U of *E. coli* ligase and 0.05% BSA were added. Then, the mixture was maintained at 37 °C for 45 min to prepare the circular PLP. Subsequently, 10 U of each exonuclease I and exonuclease III were added to the ligation mixture at 37 °C for 30 min to remove the unligated PLPs and excess linear oligonucleotides in a 40 μL reaction mixture (67 mM glycine-KOH (pH 9.5), 6.7 mM $MgCl_2$, and 1 mM dithiothreitol (DTT)). The reaction in the mixture was terminated by heating at 95 °C for 5 min.

Preparation of CP-modified MBs (CP-MBs)

After three washes, the spherical streptavidin-coated MBs were resuspended in 2X binding and washing (B&W) buffer (10 mM Tris-HCl (pH 7.5), 1 mM EDTA and 2 M NaCl) to a concentration of 5 μg/μl for immobilization. Then, 50 μL of biotinylated CP (1 μM) was incubated with 50 μL of MB suspension for 15 min at room temperature with gentle rotation. The biotinylated CPs were immobilized on MBs through the streptavidin-biotin interaction in 1X B&W buffer. Next, the CP-MBs were separated from the solution by applying a magnet for 2 min and washed three times with 1X B&W buffer. Finally, the CP-MBs were resuspended in 50 μL of deionized water for downstream use.

Solid-phase RCA on MBs

Before amplification, 2 μL of CP-MBs (1 μM) was added to two microcentrifuge tubes, each containing 20 μL of ligation and exonuclease products (circular PLPs). After the hybridization between CP and circular PLP at 37 °C for 30 min was complete, the CP-MBs were washed twice with deionized water to remove unhybridized oligonucleotides on the MB surface. Then, solid-phase RCA was performed in a 30 μL reaction mixture (10 U of Phi 29 DNA polymerase, 2 μL of 10 mM dNTPs, 33 mM of Tris-acetate (pH 7.9), 10 mM of Mg-acetate, 66 mM of K-acetate, 0.1% Tween 20, and 1 mM of DTT). After 40 min of amplification (optimized in our previous SPR biosensors), the MBs with immobilized RCA products were washed twice and resuspended in the same volume of deionized water for subsequent THz measurements.

Zeta potential measurements and confocal microscopy

For zeta potential measurements, 10 μg of different MBs at each of the steps were washed twice thoroughly, resuspended in 1 mL of deionized water and vortexed. Zeta potential measurements were conducted on a Malvern Zetasizer Nano-ZS analyzer. Prior to confocal microscopy analysis, the MBs with immobilized RCA products were washed with deionized water, incubated with SYBR Green II dye for 10 min in the dark at room temperature and then examined using a Zeiss LSM 780 confocal microscope (Carl Zeiss, Inc.).

Bacterial DNA extraction

Three species of bacteria including the target *E. coli* and two interfering bacteria, *A. baumannii* and *P. aeruginosa*, were cultured on blood agar plates (CNA, Pang Tong, Chongqing, China) overnight at 37 °C in an atmosphere containing 5% CO_2. Single bacterial colonies were harvested and suspended in sterile normal saline to an optical density of 1.0 at 600 nm. Then, bacterial genomic DNA was extracted from the bacterial suspensions using TaKaRa MiniBEST Bacteria Genomic DNA Extraction Kit Ver. 3.0. Subsequently, bacterial genomic DNA was fragmented by digestion in a 50 μL reaction mixture (1 μL of *Bam*HI, 1 μL of *Eco*RI, 1 μL of *Hin*dIII, and 1X QuickCut Buffer) at

37 °C for 10 min.[22] Then, desired concentrations of the fragmented bacterial genomic DNA were prepared in deionized water and detected according to the aforementioned protocol.

THz instrumentation and sample cell

The THz spectroscopic measurements in this study were conducted on a commercial THz time-domain spectroscopy system in transmission mode (TAS7500SP, Advantest). Details of this system regarding the element technology and data analysis have been previously described.[23-25] Briefly, two synchronized control mode-locked optical fibre lasers (λ=1550 nm; pulse width, ~40 fs) were used as a pump and a probe pulse, respectively. A time-domain THz pulse was emitted when the pump pulse was focused on the biased GaAs photoconductive antenna. Subsequently, the THz pulse was collimated on the sample by two parabolic mirrors to obtain the sample THz waveform, while the probe pulse was directly detected by the photoconductive antenna detector for the reference signal.[26] As a result, time-resolved spectroscopic analysis of the sample could be realized by controlling the delay between the pump and probe pulses. The observed frequency range was 0.1 to 2 THz in this study with a frequency resolution of 7.6 GHz.

A fluidic chip composed of two optical windows was used as the sample cell for THz measurements. To decrease the attenuation of THz energy, the THz absorption coefficients of four candidate windows fabricated using different materials (polydimethylsiloxane (PDMS), quartz, COP (cyclo-olefin polymer) and PE (polyethylene)) were compared (Fig. S1). A lower THz absorption was observed for PE and COP than for PDMS and quartz, but PE was opaque to visible light. Therefore, the COP window was chosen to prepare the fluidic chip to more conveniently assess the sample loading. The designed structure for sample storage in the fluidic chip has a floor area of 52.5 mm^2 to match the spot size and a depth of 80 μm (the optical path of THz radiation), so the minimal volume required to completely fill the structure with a

sample is approximately 4.2 μL. An image of the fluidic chip (Fig. S2) and the fabrication process can be found in the supplementary information.

Measurement

The experimental measurements were conducted at a room temperature of 22 ± 0.3 °C with a purge of dry nitrogen gas to eliminate the THz absorption from water vapour. All samples were mixed thoroughly before they were injected into the fluidic chip to ensure that the MBs were evenly dispersed in the solutions. A blank fluidic chip was measured as a reference to calculate the THz response of all the samples. After the THz measurements were performed, the frequency domain data were obtained from the time-domain spectra via Fourier transform. To facilitate a comparison, the reflection and scattering losses of THz radiation were ignored so that the absorption coefficients (α) of the samples could be calculated according to the Beer-Lambert law:[27]

$$\alpha(f) = \frac{\ln I_r(f) - \ln I_s(f)}{d} \quad (1)$$

where d is the thickness of the sample, f is the frequency, and $I_r(f)$ and $I_s(f)$ are the power transmissions of the samples and the blank fluidic chip, respectively. After calculation, a simple adjacent averaging method was used to smooth the data.[28]

Results and discussion

Solid-phase RCA on MBs

As illustrated in Fig. 1, this detection protocol primarily includes three steps: (i) PLP circularization upon recognition of the target sequence in solution, which was realized by the ligation of their complementary sequences at the 5' and 3' ends (the underlined sequences in Table 1); (ii) hybridization between the CPs immobilized on MBs and the circular PLPs followed by the signal amplification via RCA; and (iii) magnetic separation of RCA products for THz measurements. In contrast, the PLPs could not hybridize with the control sequence, and the non-circularized PLPs were removed by

the subsequent exonuclease treatment; thus, no amplification template remained for RCA. The details for selecting this *E. coli*-specific target sequence and for designing its complementary PLP can be found in our previous report.[12]

The purpose of this study was to employ THz spectroscopy to detect amplified DNA products on MBs; thus, the solid-phase RCA on MBs was validated first. To evaluate the RCA reaction performance, ligation products and RCA products were analysed by 2% agarose gel electrophoresis. As shown in Fig. 2A, the circular PLP migrated at a slower rate than the linear PLP and the target sequence, illustrating the effective circularization of the linear PLP upon recognition of the target sequence. In addition, since RCA continuously produced high-molecular-mass, single-stranded DNA composed of tandem-repeat copies of the circular PLP, the RCA products were too large to enter the gels (Fig. 2B). To further validate the RCA reaction that occurred on the MB surface, MBs immobilized with RCA products (RCA-MBs) were characterized by both zeta potential and confocal microscopy. Zeta potential measurements provide surface information, including the surface charge and chemical modifications of nano- and microparticles, with minimal sample preparation.[29, 30] As observed in Fig. 2C, the zeta potential of blank MB (without CP) was similar to that of CP-MB (-29.7±0.15 mV vs. -28.6±0.25 mV). The slight shift of approximately 1 mV to more positive values may be attributed to the blocking effect of the negatively charged MB surface by short CPs with less negative charges. However, an obvious shift to more negative values was observed for RCA-MB (-42.9±0.90 mV), indicating the coverage of the MBs with amplified DNA products (possessing more negative charges), which is in accordance with the previous observation on amplified DNA labelled with gold nanoparticles.[31] This evidence was also corroborated by confocal microscopy images (Fig. 2D and 2E). For RCA-MB, the amplified DNA products on MBs were stained green with SYBR Green II fluorescent dye, while no fluorescence staining was observed for the CP-MBs. The green area indicates that all the RCA products were bound to the surface of MBs. In accordance with this observation, a previous study of solid-phase RCA on Sepharose beads also illustrated that DNA products could be

stained as 1-μm-sized fluorescent spots on the bead surface using complementary fluorescent probes.[32] Therefore, the amplification effectiveness was demonstrated as a prerequisite for the subsequent THz measurements.

THz measurements of different MB suspensions

First, different amplified MB suspensions were measured using THz spectroscopy before and after magnetic separation. Fig. 3A shows the power of the transmitted THz pulses for RCA-MB in water, RCA-MB in sample matrix, negative MB amplified with the control sequence (NTC-MB) in water, NTC-MB in sample matrix, and water. The lowest power of water demonstrates its highest absorption in the THz range. Before magnetic separation was applied, RCA-MB in sample matrix (black curve) and NTC-MB in sample matrix (red curve) only slightly differed due to the complex sample matrix components. Their differences in the RCA products immobilized on MBs were substantially masked by the THz absorption of other components in the sample matrix (dNTPs, ions, enzyme and buffer). After being magnetically separated and resuspended in the same volume of water, RCA-MB displayed the lowest THz absorption due to the amplified DNA products. In contrast, NTC-MB without significant amplification displayed a much higher THz absorption. Therefore, the magnetic separation of DNA products is necessary to remove interferences from the sample matrix for THz measurements.

Fig. 3B shows the comparative absorption coefficients of water and three MB suspensions: blank MB, NTC-MB, and RCA-MB. The difference in the absorption coefficients between water and blank MB was negligible compared to that of water and the other two MB suspensions. Therefore, the MBs should not significantly change the overall THz absorption of suspensions, and the observed differences among the suspensions were due to the DNA molecules, which have much lower absorption. More specifically, the obvious difference between water and RCA-MB was due to the amplified DNA products on the surface of the MBs, while a much smaller difference

between water and NTC-MB could be attributed to the limited RCA-free extension from the unligated PLP.[12, 13]

Sensitivity of target sequence detection

After an illustration of the detection principle, the sensitivity of this method for target sequence detection was evaluated using 100 nM PLP. As shown in Fig. 4A, as the concentration of the target sequence increased, the absorption coefficients of the RCA-MB suspensions decreased. To further investigate these concentration-dependent changes, the average differences in the absorption coefficients between water and RCA-MB suspensions ($\Delta\alpha = \alpha_{water} - \alpha_{sample}$) from 0.8 to 1.2 THz were calculated. The analytical signals were linear with the logarithm of the target sequence concentration over the range from 10^{-10} M to 10^{-7} M ($y=14.8x+156.9$, $R^2=0.9639$) (Fig. 4B). Meanwhile, the detection limit of this method was estimated to be 0.6×10^{-10} M, which gives a signal that is higher than the blank signal plus 3 times its standard deviation (SD),[31] indicating that 0.12 fmol of the target sequence can be effectively detected in a 30 μL reaction mixture containing 2 μL of the target sequence. Although the sensitivity of the current assay (0.06 nM) is lower than that of our previous SPR biosensor coupled with gold nanoparticles for signal amplification,[12] this value is comparable to or even exceeds similar reported methods for DNA detection, such as electrochemical detection based on RCA (0.1 nM),[33] piezoelectric detection based on a DNA ligase reaction (2.6 nM),[34] a film bulk acoustic resonator (FBAR) sensor based on binding probes (1 nM),[35] and SPR detection based on surface hybridization (5 nM).[36] This sensitivity should be attributed to the unique ability of THz spectroscopy to measure low-frequency biomolecular motions and non-bonded (hydrophobic) interactions originating from the DNA molecules in suspensions; thus, the corresponding miniscule structural changes around the MBs after amplification can be effectively probed. Furthermore, the reproducibility of this method was evaluated by the relative standard deviation (RSD) values of five replicates at different concentrations: 6.9% at 10^{-9} M, 5.4% at 10^{-8} M and 5.8% at 10^{-7} M, suggesting an acceptable reproducibility.[37]

These results can be explained by the widely known concept of 'THz defect' in the THz community, meaning that biomolecules alone absorb much less THz radiation than water, so the absorption of the corresponding biomolecule solution decreases linearly with the increasing solute concentration.[1, 38, 39] In addition to nucleic acids,[7] the THz absorption coefficients of red blood cells (RBCs) in both normal saline and whole blood were also shown to vary linearly with the RBC concentration.[40] In that study, the excellent linear relationship between the RBC concentration and the THz signals at different frequencies provided a basis for quantitative blood analysis by THz spectroscopic imaging. In contrast, a non-linear behaviour of THz absorption with respect to the solute concentration has also been observed for some proteins and carbohydrates.[6, 41, 42] This phenomenon can be explained by the other concept of 'THz excess', indicating that a strongly absorbing hydration shell in the solute-water mixture overcompensates for the decreased absorption caused by water replacement under dilute conditions but overlaps at a certain concentration, thus causing a non-linear behaviour.[39, 43] Nevertheless, it is too complicated to speculate the exact concentration-dependent behaviour of the RCA products that are immobilized on MBs since the behaviour should also be closely related to the THz frequencies and product concentrations. Considering the size similarity between RBCs and RCA-MBs (Fig. 2D), the linear decrease in the THz absorption coefficients with increasing target sequence concentration should be theoretically possible.

Detection of bacterial genomic DNA

After the previous sensitivity investigation, bacterial genomic DNA was analysed using the current assay to demonstrate its utility. To evaluate the sensitivity of the assay for genomic DNA detection, serially diluted *E. coli* samples were analysed using a fixed concentration of PLP (100 nM). Similar to the synthetic target sequence, the analytical THz signals of genomic DNA also displayed a linear relationship with the logarithm of the genomic DNA concentration over the range of 0.05-1 ng/μl ($y=22.3x+34.9$, $R^2=0.9615$) (Fig. 5). This linear fit is different from that of the target sequence due to the lower capture and hybridization efficiency, which results from the clearly greater

steric hindrance. Meanwhile, the detection limit of the proposed strategy for bacterial genomic DNA detection was estimated to be 0.05 ng/μl. Although this value was marginally inferior to the detection limits of other isothermal amplification assay platforms, such as electrochemical detection combined with thermophilic helicase-dependent isothermal amplification (0.01 ng/μl)[44] and the colorimetric loop-mediated isothermal amplification (LAMP) assay (100 fg/tube),[45] the proposed method still possesses several advantages, such as a moderate reaction temperature, contamination resistance, and simple operation without a complicated primer design. Meanwhile, further studies could be envisioned to use magnetic nanoparticles with less steric hindrance and a settling effect for more efficient hybridization with the target sequence in genomic DNA.

To evaluate the specificity of the current assay, bacterial genomic DNA samples extracted from the target *E. coli* and two interfering bacteria, *A. baumannii* and *P. aeruginosa*, were detected according to the aforementioned protocol. As shown in Fig. 6, the average difference in absorption coefficients of the *E. coli* sample relative to water (39.4±4.0 cm^{-1}) was significantly higher than that of the *P. aeruginosa* sample (5.2±1.3 cm^{-1}) and the *A. baumannii* sample (5.0±1.1 cm^{-1}) ($p<0.05$). In addition, a mixture of the *P. aeruginosa* and *A. baumannii* samples (Mixture 1) and a mixture of all samples (Mixture 2) were also investigated. Mixture 1 displayed no difference compared to the separate *A. baumannii* and *P. aeruginosa* samples (5.5±1.3 cm^{-1}), while a minor decrease of 7.6% was observed for Mixture 2 compared to the *E. coli* sample. Then, the degree of interference (DI) of the interfering bacteria could be calculated using equation,[46]

$$\mathrm{DI} = \frac{I-B}{E-B} \times 100\% \quad (2)$$

where *I*, *B* and *E* represent the average differences in absorption coefficients relative to water of the interfering bacteria, the blank sample and *E. coli*, respectively. The DI values of the two interfering bacteria and Mixture 1 were all below 5% (3.3% for *P. aeruginosa*, 2.7% for *A. baumannii* and 4.0% for Mixture 1), demonstrating the specificity of the current assay for *E. coli* detection. This property should be primarily

attributed to the high specificity of hybridization and ligation in solution, where PLP only circularized in the presence of the target sequence. Additionally, MBs were utilized to magnetically purify the RCA products to decrease the background signal by removing the limited nonspecific DNA amplification and adhesion on the surface of MBs, thus ensuring detection specificity.

Conclusion

In summary, we demonstrated the first combination of DNA biosensing by THz spectroscopy, target sequence amplification by RCA and rapid magnetic separation by MBs. Using *E. coli* as the model, a new strategy for the isothermal detection of bacterial DNA was proposed. The detection principle was based on the much lower THz absorption of nucleic acids than water molecules, and a linear relationship between the analytical THz signals of RCA-MB suspensions and the target sequence concentration was observed. By exploiting the intrinsically high sensitivity of THz spectroscopy and RCA, 0.12 fmol of synthetic bacterial DNA and 0.05 ng/μl of genomic DNA were detected using the proposed strategy with high specificity. CP-labelled MBs were used as the solid-phase RCA reaction support to facilitate the rapid magnetic purification of DNA products for direct THz measurements, without requiring an extra hybridization procedure. Compared to similar reported methods, the proposed strategy exhibits several advantages, such as simplicity, rapidity, small sample volume and low power consumption. Based on these findings, a multifunctional assay platform for multiplex detection of pathogenic bacteria can be developed by integrating MB-based RCA with microfluidic chip technology, such that assay procedures including the RCA reaction, product purification and THz measurements can be successively conducted in a separate microchamber. Furthermore, we hope this proof-of-concept demonstration could present a general methodology of DNA biosensing using THz spectroscopy, as the selectivity principle can be easily extended to probe other DNA targets using the complementary PLP specific to the target sequence.

View Article Online
DOI: 10.1039/C7AN01438D

Conflicts of interest

There are no conflicts of interest to declare.

Acknowledgements

This work was partially supported by the National Basic Research Program of China (2015CB755400), the National Natural Science Foundation of China (81430054, 81370049), and Major Project of Military Science and Technology (BWS13C013).

References

1. F. Shuting, H. Yuezhi, S. U. Benjamin and P.-M. Emma, *Journal of Physics D: Applied Physics*, 2014, **47**, 374009.
2. X. Yang, X. Zhao, K. Yang, Y. Liu, Y. Liu, W. Fu and Y. Luo, *Trends in Biotechnology*, 2016, **34**, 810-824.
3. H.-B. Liu, G. Plopper, S. Earley, Y. Chen, B. Ferguson and X. C. Zhang, *Biosens. Bioelectron.*, 2007, **22**, 1075-1080.
4. B. Born, H. Weingaertner, E. Bruendermann and M. Havenith, *J. Am. Chem. Soc.*, 2009, **131**, 3752-3755.
5. Y. C. Shen, *Int. J. Pharm.*, 2011, **417**, 48-60.
6. Y. Sun, Y. Zhang and E. Pickwell-MacPherson, *Biophys. J.*, 2011, **100**, 225-231.
7. A. Arun, L. Trung Quan, K. Matthias, K. Young Jun, N. Chang-Hoon, M. Andreas and H. Martina, *Analyst*, 2012, **137**, 575-579.
8. M. Heyden and M. Havenith, *Methods*, 2010, **52**, 74-83.
9. M. M. Ali, F. Li, Z. Zhang, K. Zhang, D.-K. Kang, J. A. Ankrum, X. C. Le and W. Zhao, *Chemical Society Reviews*, 2014, **43**, 3324-3341.
10. T. Kobori and H. Takahashi, *Anal. Sci.*, 2014, **30**, 59-64.
11. T. Konry, I. Smolina, J. M. Yarmush, D. Irimia and M. L. Yarmush, *Small*, 2011, **7**, 395-400.
12. D. Shi, J. Huang, Z. Chuai, D. Chen, X. Zhu, H. Wang, J. Peng, H. Wu, Q. Huang and W. Fu, *Biosens. Bioelectron.*, 2014, **62**, 280-287.
13. Y. Xiang, K. Deng, H. Xia, C. Yao, Q. Chen, L. Zhang, Z. Liu and W. Fu, *Biosens. Bioelectron.*, 2013, **49**, 442-449.

14. P. A. George, W. Hui, F. Rana, B. G. Hawkins, A. E. Smith and B. J. Kirby, *Opt. Express*, 2008, **16**, 1577-1582.
15. J. B. Masson, M. P. Sauviat, J. L. Martin and G. Gallot, *Proc. Natl. Acad. Sci. U.S.A*, 2006, **103**, 4808-4812.
16. Evangelos Zoidis, ‡, Jack Yarwood, † And and M. Besnard‡, *J. Phys. Chem. A* 1999, **103**, 220-225.
17. S. Funkner, G. Niehues, D. A. Schmidt, M. Heyden, G. Schwaab, K. M. Callahan, D. J. Tobias and M. Havenith, *J. Am. Chem. Soc.*, 2012, **134**, 1030-1035.
18. Q. Su, D. Xing and X. Zhou, *Biosens. Bioelectron.*, 2010, **25**, 1615-1621.
19. B. D. Plouffe, S. K. Murthy and L. H. Lewis, *Reports on Progress in Physics*, 2015, **78**, 016601.
20. J. Lee, K. Icoz, A. Roberts, A. D. Ellington and C. A. Savran, *Anal. Chem.*, 2010, **82**, 197-202.
21. L. Zuccaro, C. Tesauro, B. Cerroni, A. Ottaviani, B. R. Knudsen, K. Balasubramanian and A. Desideri, *Analytical Biochemistry*, 2014, **451**, 42-44.
22. M. Szemes, P. Bonants, M. de Weerdt, J. Baner, U. Landegren and C. D. Schoen, *Nucleic Acids Research*, 2005, **33**, e70.
23. K. Shiraga, H. Naito, T. Suzuki, N. Kondo and Y. Ogawa, *Journal of Physical Chemistry B*, 2015, **119**, 5576-5587.
24. L. Jiang, M. Li, C. Li, H. Sun, L. Xu, B. Jin and Y. Liu, *J. Infrared Millim. Te.*, 2014, **35**, 871-880.
25. J. Qin, L. Xie and Y. Ying, *Food Chem.*, 2017, **224**, 262-269.
26. K. Shiraga, T. Suzuki, N. Kondo, T. Tajima, M. Nakamura, H. Togo, A. Hirata, K. Ajito and Y. Ogawa, *J. Chem. Phys.*, 2015, **142**, 6536-6205.
27. S. Yan, D. Wei, M. Tang, C. Shi, M. Zhang, Z. Yang, C. Du and H.-L. Cui, *IEEE Trans. THz Sci. Technol.*, 2016, **6**, 532-540.
28. X. Yang, D. Wei, S. Yan, Y. Liu, S. Yu, M. Zhang, Z. Yang, X. Zhu, Q. Huang, H.-L. Cui and W. Fu, *J. Biophotonics*, 2016, **9**, 1050-1058.
29. Y. Zhang, M. Yang, N. G. Portney, D. Cui, G. Budak, E. Ozbay, M. Ozkan and C. S. Ozkan, *Biomedical Microdevices*, 2008, **10**, 321-328.
30. F. Thielbeer, K. Donaldson and M. Bradley, *Bioconjugate Chemistry*, 2011, **22**, 144-150.
31. A. de la Escosura-Muniz, L. Baptista-Pires, L. Serrano, L. Altet, O. Francino, A. Sanchez and A. Merkoci, *Small*, 2016, **12**, 205-213.
32. K. Sato, A. Tachihara, B. Renberg, K. Mawatari, K. Sato, Y. Tanaka, J. Jarvius, M. Nilsson and T. Kitamori, *Lab on a Chip*, 2010, **10**, 1262-1266.

33. S. Zhang, Z. Wu, G. Shen and R. Yu, *Biosens. Bioelectron.*, 2009, **24**, 3201-3207.
34. L. Pang, J. Li, J. Jiang, G. Shen and R. Yu, *Analytical Biochemistry*, 2006, **358**, 99-103.
35. S. Auer, M. Nirschl, M. Schreiter and I. Vikholm-Lundin, *Analytical and Bioanalytical Chemistry*, 2011, **400**, 1387-1396.
36. A. Rachkov, S. Patskovsky, A. Soldatkin and M. Meunier, *Talanta*, 2011, **85**, 2094-2099.
37. Y. Xiang, X. Zhu, Q. Huang, J. Zheng and W. Fu, *Biosens. Bioelectron.*, 2015, **66**, 512-519.
38. D. M. Leitner, M. Gruebele and M. Havenith, *Hfsp Journal*, 2008, **2**, 314-323.
39. B. Born and M. Havenith, *J. Infrared Millim. Te.*, 2009, **30**, 1245-1254.
40. K. Jeong, Y. M. Huh, S. H. Kim, Y. Park, J. H. Son, S. J. Oh and J. S. Suh, *J. Biomed. Opt.*, 2013, **18**, 107008.
41. B. Born, S. J. Kim, S. Ebbinghaus, M. Gruebele and M. Havenith, *Faraday Discuss.*, 2009, **141**, 161-173.
42. M. Heyden, E. Bruendermann, U. Heugen, G. Niehues, D. M. Leitner and M. Havenith, *J. Am. Chem. Soc.*, 2008, **130**, 5773-5779.
43. V. C. Nibali and M. Havenith, *J. Am. Chem. Soc.*, 2014, **136**, 12800-12807.
44. E. Torres-Chavolla and E. C. Alocilja, *Biosens. Bioelectron.*, 2011, **26**, 4614-4618.
45. X. Zhao, L. Wang, Y. Li, Z. Xu, L. Li, X. He, Y. Liu, J. Wang and L. Yang, *World Journal of Microbiology & Biotechnology*, 2011, **27**, 181-184.
46. Y. He, M. Wang, E. Fan, H. Ouyang, H. Yue, X. Su, G. Liao, L. Wang, S. Lu and Z. Fu, *Anal. Chem.*, 2017, **89**, 1916-1921.

View Article Online
DOI: 10.1039/C7AN01438D

Table

Table 1. Oligonucleotide sequences used in this study

Oligonucleotide	Sequence (5'-3')
Padlock probe	Phosphate-CTGTTACCGTTCGACTTGCATG**AGCACCAATAGTCTTCAGTTC**ACATCAAATGCCACGTTAACAGTCAGGCCTAGCAAGCTTCTTC
Target sequence	AGGCCTAACACATGCAAGTCGAACGGTAACAGGAAGAAGCTTGCTTCTTTGCTGA
Capture probe	Biotin-$(CH_2)_6$-TTTTTTTTTT**GAACTGAAGACTATTGGTGCT**
Control sequence	AGGCCTAACACACATAGACTAGGTAACGGTGAAGGAGGATCCATCTCTTTGCTGA

The sequence underlined in the padlock probe (PLP) matches the underlined sequence in the target sequence, and the bold sequence in the PLP is complementary to the bold sequence in the capture probe (CP). A non-complementary sequence to the PLP was used as a control sequence. The CP was labelled with biotin for biotin-streptavidin linkage to the magnetic beads (MBs).

View Article Online
DOI: 10.1039/C7AN01438D

Figure

Figure captions

Fig. 1 Schematic description of THz spectroscopy for bacterial DNA detection by MB-based RCA

Fig. 2 Characterization of solid-phase RCA on MBs. (A) Electrophoretic identification of the ligation reaction mixture. Lanes 1, 2, 3 and 4 represent the blank control, linear PLP, target sequence and ligation products, respectively. High concentrations of oligonucleotides (1 μM) were used for better illustration. (B) Electrophoretic identification of the RCA products. Lanes 1 and 2 represent the blank control and amplified DNA products, respectively. (C) Zeta potential of MBs at different steps: blank MB, CP-MB and RCA-MB. Error bars indicate the SD (n=3). (D) Confocal microscopy image of the RCA-MBs. (E) Confocal microscopy image of the CP-MBs.

Fig. 3 THz measurements of different MB suspensions. (A) Power spectra of RCA-MB and NTC-MB suspensions and water. The inset graph shows a magnification of the signal from 0.8 to 0.9 THz. (B) Absorption coefficients of water and different MB suspensions. The inset graph shows a magnification of the signal from 0.8 to 0.9 THz.

Fig. 4 Evaluation of the sensitivity of target sequence detection. (A) Absorption coefficients of water and RCA-MB suspensions amplified with different concentrations of the synthetic target sequence. (B) Average differences in the absorption coefficients between water and RCA-MB suspensions (Δα) from 0.8 to 1.2 THz with respect to the target sequence concentration. The inset graph corresponds to the relationship between the analytical signal and the logarithm of the target sequence concentration. Error bars indicate the SD (n=5).

Fig. 5 Evaluation of the sensitivity of genomic DNA detection. The inset graph corresponds to the relationship between the analytical signal (Δα) and the logarithm of the genomic DNA concentration. Error bars indicate the SD (n=5).

Fig. 6 Assessment of the specificity of bacterial DNA detection. Mixture 1 was composed of *P. aeruginosa* and *A. baumannii* DNA samples, and Mixture 2 was composed of all bacterial DNA samples. Error bars indicate the SD (n=5).

View Article Online
DOI: 10.1039/C7AN01438D

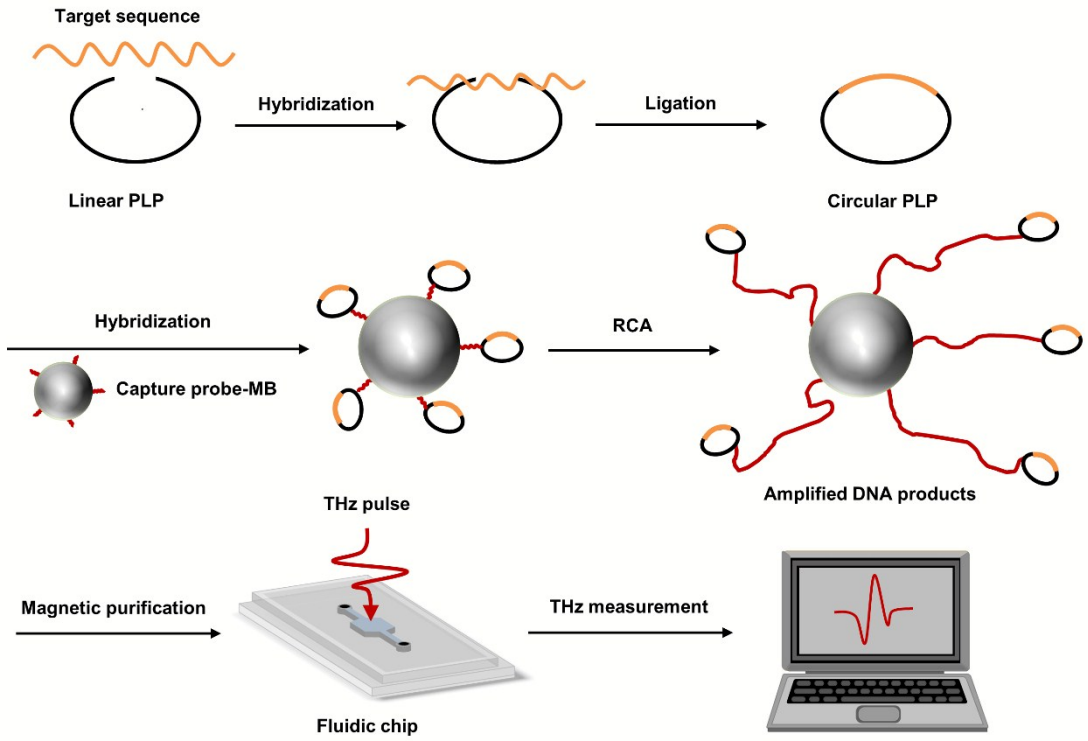

Fig. 1

View Article Online
DOI: 10.1039/C7AN01438D

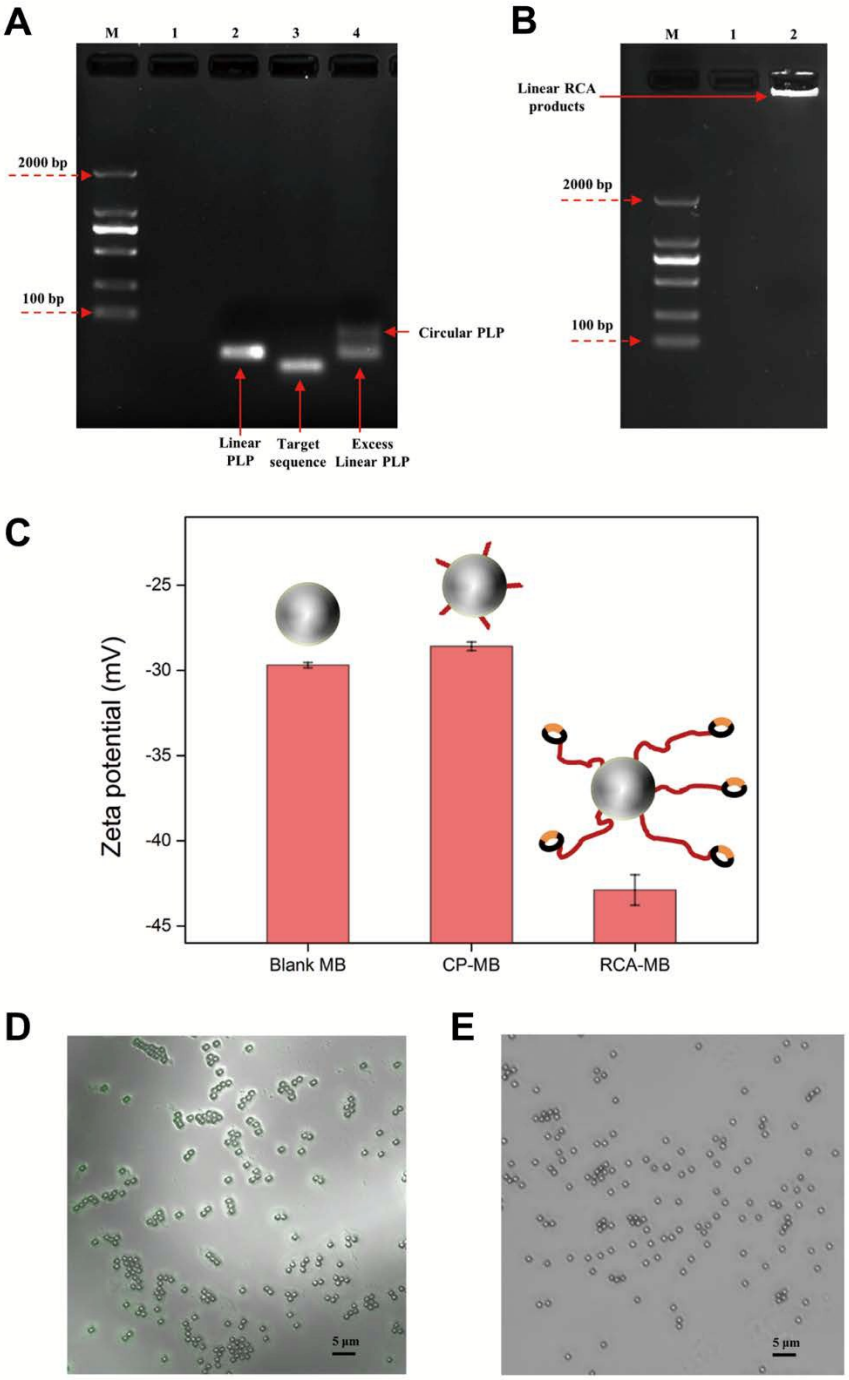

Fig. 2

View Article Online
DOI: 10.1039/C7AN01438D

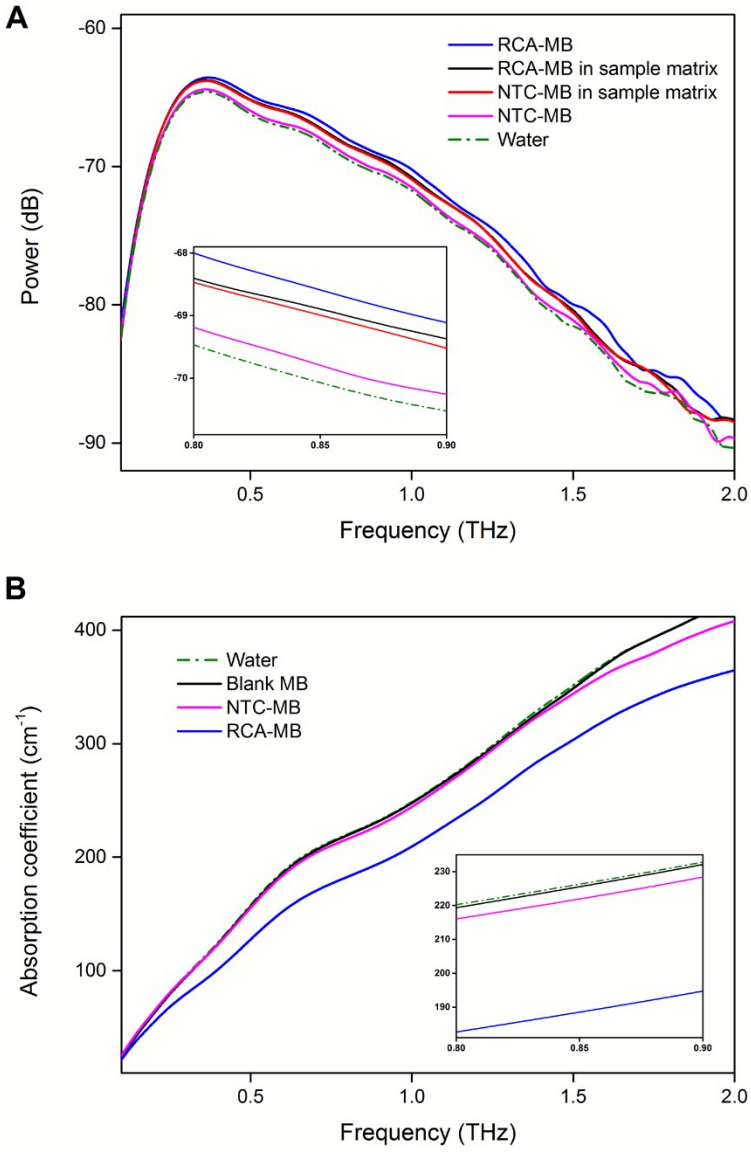

Fig. 3

View Article Online
DOI: 10.1039/C7AN01438D

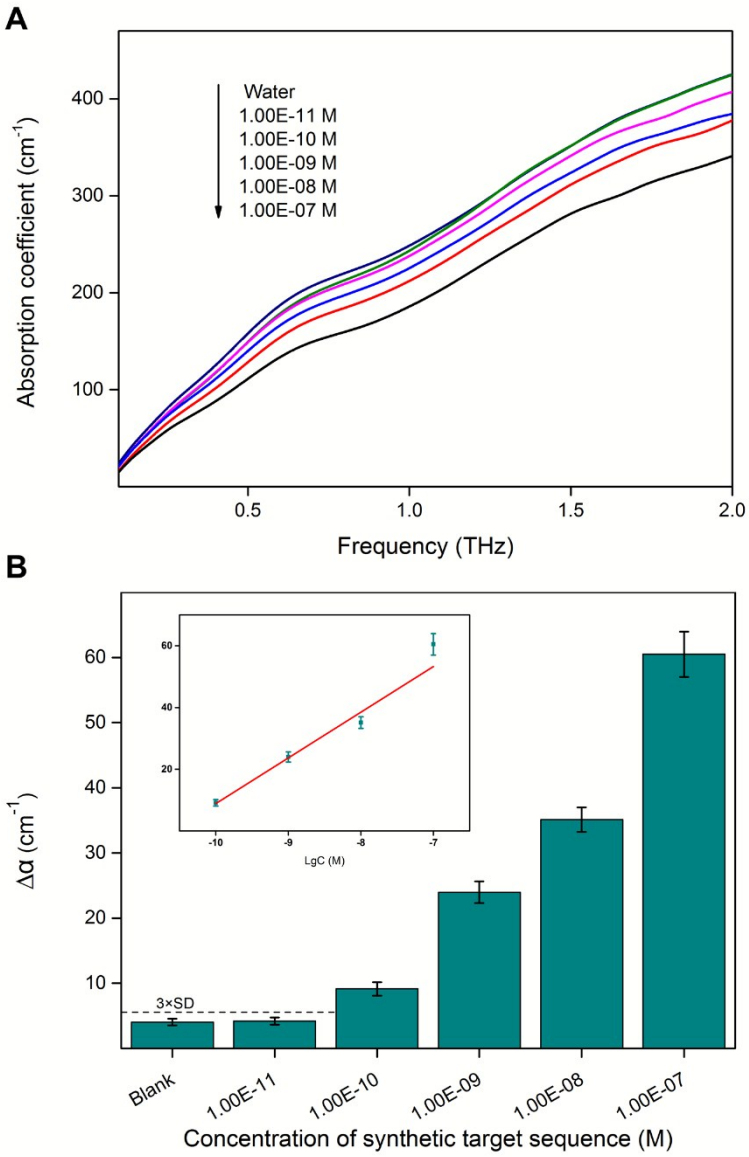

Fig. 4

View Article Online
DOI: 10.1039/C7AN01438D

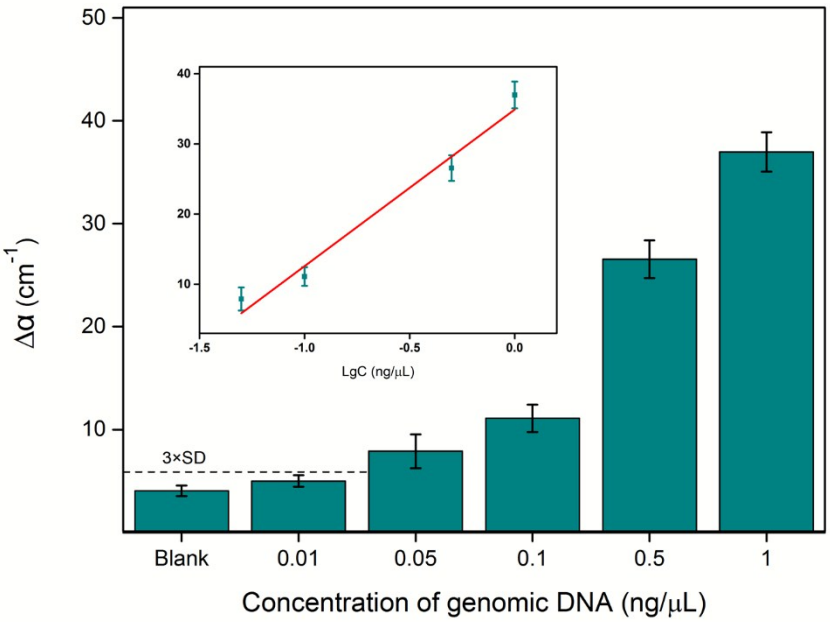

Fig. 5

View Article Online
DOI: 10.1039/C7AN01438D

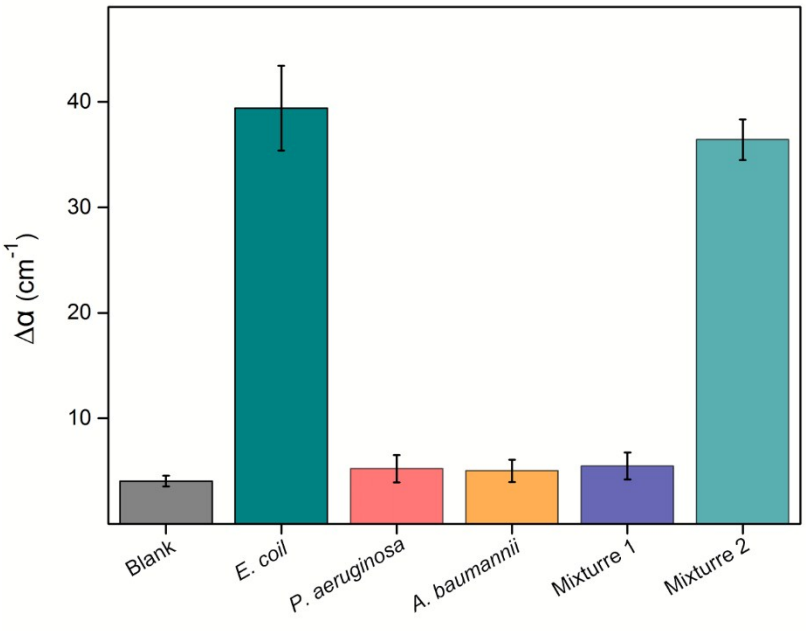

Fig. 6

View Article Online
DOI: 10.1039/C7AN01438D

TOC

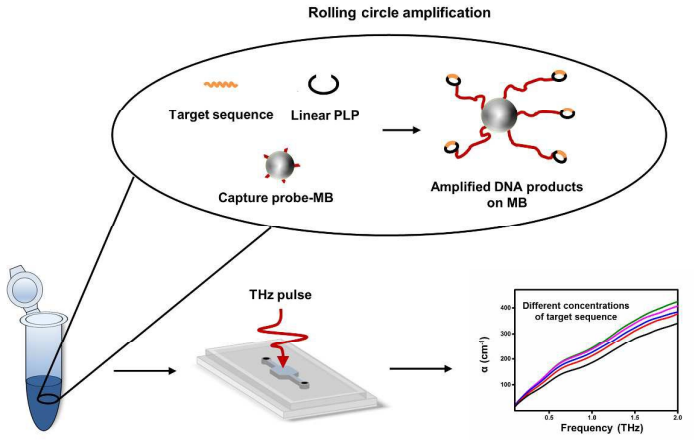

A terahertz biosensor based on rolling circle amplification was developed for the isothermal detection of bacterial DNA.

View Article Online
DOI: 10.1039/C7AN01438D

Supplementary information

Terahertz spectroscopy for the isothermal detection of bacterial DNA by magnetic bead-based rolling circle amplification

Xiang Yang, Ke Yang, Xiang Zhao, Zhongquan Lin, Zhiyong Liu, Sha Luo, Yang Zhang, Yunxia Wang, Weiling Fu*

Department of Laboratory Medicine, Southwest Hospital, Third Military Medical University, Chongqing 400038, China

Corresponding Author

*(W.-L.F) E-mail: weiling_fu@126.com

View Article Online
DOI: 10.1039/C7AN01438D

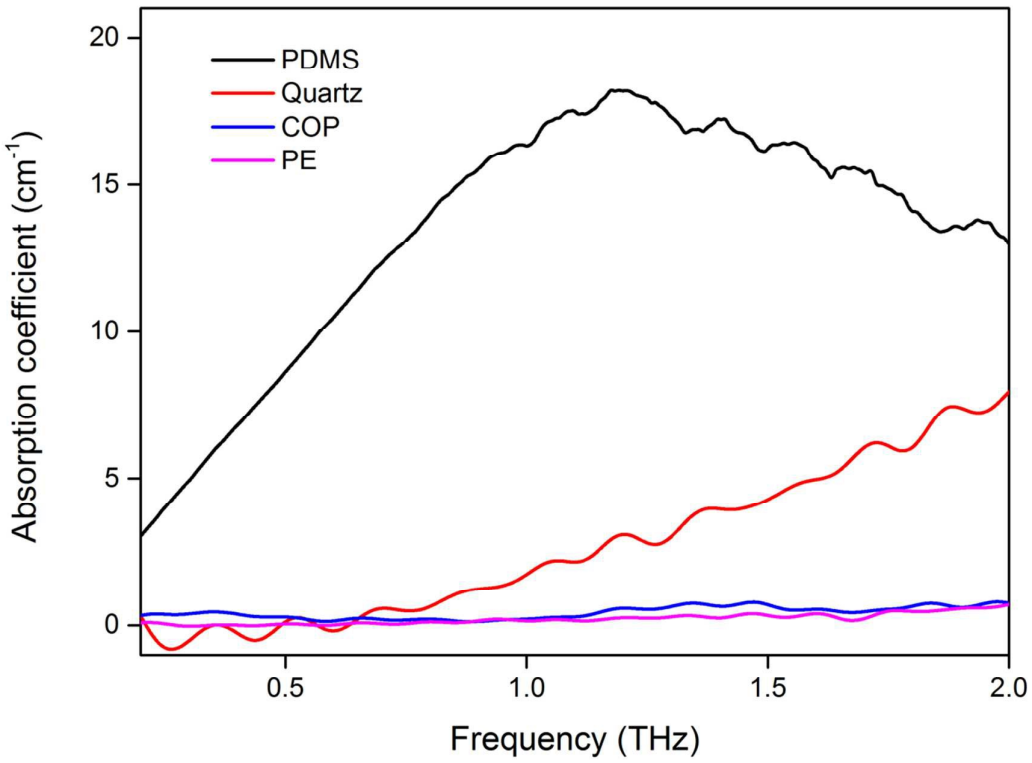

Figure S1. Comparison of the absorption coefficients of PDMS, quartz, COP and PE

View Article Online
DOI: 10.1039/C7AN01438D

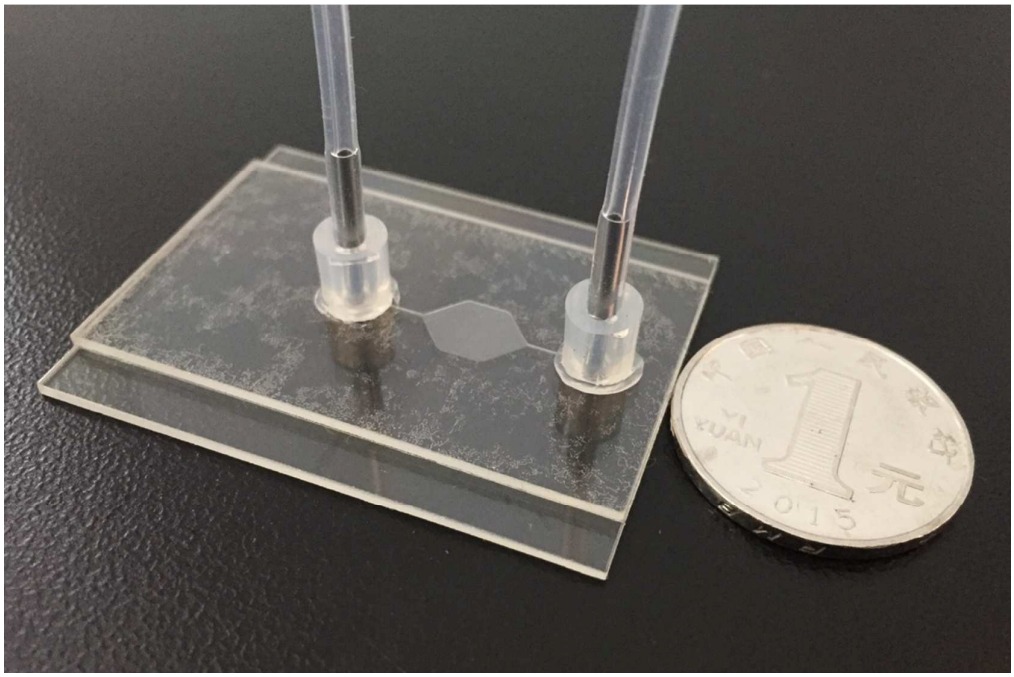

Figure S2. Image of the fluidic chip. The size of the lower layer was designed to be compatible with the sample holder of the THz spectrometer so that the fluidic chip can be directly inserted into the sample chamber after sample loading.

View Article Online
DOI: 10.1039/C7AN01438D

Experimental

The fabrication of the fluidic chip mainly included three steps: (i) cutting two COP layers of different sizes (30×50×1 mm and 40×50×1 mm) to prepare the upper layer and lower layer of the chip by a computerized numerically controlled machine; (ii) using a piece of PET-based, double-sided adhesive layer to adhere the lower COP layer, and processing the designed structure for sample storage and a channel of 0.2 mm width by a high-speed milling cutter; (iii) bonding and heating two COP layers on a hot plate to a certain high temperature to form a total thickness of 2.08 mm. Therefore, the fixed PET layer with a thickness of 80 μm placed between two parallel COP windows was the sample thickness of the fluidic chip.